JACS
JOURNAL OF THE AMERICAN CHEMICAL SOCIETY
Communication
pubs.acs.org/JACS

Probing Spatial Organization of DNA Strands Using Enzyme-Free Hairpin Assembly Circuits

Bingling Li, Yu Jiang, Xi Chen,* and Andrew D. Ellington*

Institute for Cellular and Molecular Biology, Center for Systems and Synthetic Biology, Department of Chemistry and Biochemistry, University of Texas at Austin, Austin, Texas 78712, United States

Supporting Information

ABSTRACT: Catalyzed hairpin assembly (CHA) is a robust enzyme-free signal-amplification reaction that has a wide range of potential applications, especially in biosensing. Although most studies of the analytical applications of CHA have focused on the measurement of concentrations of biomolecules, we show here that CHA can also be used to probe the spatial organization of biomolecules such as single-stranded DNA. The basis of such detection is the fact that a DNA structure that brings a toehold and a branch-migration domain into close proximity can catalyze the CHA reaction. We quantitatively studied this phenomenon and applied it to the detection of domain reorganization that occurs during DNA self-assembly processes such as the hybridization chain reaction (HCR). We also show that CHA circuits can be designed to detect certain types of hybridization defects. This principle allowed us to develop a "signal on" assay that can simultaneously respond to multiple types of mutations in a DNA strand in one simple reaction, which is of great interest in genotyping and molecular diagnostics. These findings highlight the potential impacts of DNA circuitry on DNA nanotechnology and provide new tools for further development of these fields.

Although nucleic acids are best known as genetic materials, they have been engineered to perform a wide range of tasks. For example, DNAzymes and aptamers enable the detection and manipulation of biomolecules,[1] while more recently, DNA tile assembly and DNA origami have been shown to be useful for the precise positioning of molecules with subnanometer precision.[2] Enzyme-free DNA circuits have been shown to be capable computers.[3]

While the design of nucleic acid structures and circuits has proceeded quickly, the analytical methodologies capable of probing these DNA nanotechnologies have lagged. Atomic force microscopy can be used to look at the gross outline of DNA nanostructures,[2c,4] and DNA circuits can be adapted to ensemble methods for detection, such as fluorescence spectroscopy and electrochemistry.[5] However, intimate probing of individual portions of the nanostructures themselves has generally been carried out with technically demanding methods such as restriction digestion or chemical probing.[6]

In this work, we exploited the advances in DNA nanotechnology design and adapted these advances to much finer probing of structures and circuits by developing a new design principle, proximity detection within DNA nanostructures. We started with an enzyme-free signal-amplification circuit, catalyzed hairpin assembly (CHA),[3d,5a] but made the execution of this circuit dependent upon the formation of a particular nanostructure, an assembled hybridization chain reaction (HCR)[3a] concatemer, whose molecular junctions are otherwise "invisible" with extant technologies (Figure 1). The sensitivity

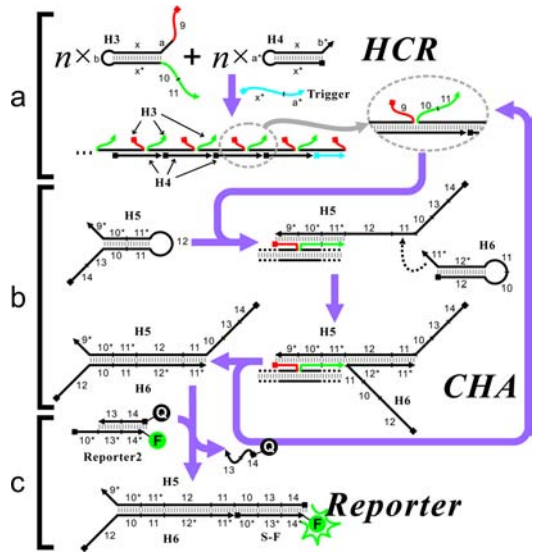

Figure 1. Scheme of the CHA-based circuit that detects the degree of HCR assembly. (a) Scheme of HCR with extended domains. (b) CHA reaction catalyzed by the correctly formed HCR product. (c) Fluorescent reporter that detects the product of the CHA reaction.

of this method is such that it can be used to probe defects in DNA nanomaterials caused by mismatches at the junctions of hybridized DNA strands. It has also proved to be a simple and effective analytical tool that allows the direct readout of HCR in homogeneous solution without the use of specialty fluorescent oligonucleotides as HCR substrates.

The scheme for proximity detection is shown in Figure 1. An HCR reaction composed of two substrate hairpin DNAs, **H3** and **H4**, is initiated by the **Trigger** strand (Figure 1a). However, in contrast to traditional HCR,[3a] in our study hairpin **H3** has been extended with a 10 nucleotide (nt) segment, "9" (Figure 1, red), at its 5′ end and an 18 nt segment, "10 + 11"

Received: January 30, 2012
Published: August 15, 2012

   dx.doi.org/10.1021/ja300984b | J. Am. Chem. Soc. 2012, 134, 13918−13921

(Figure 1, green), at its 3′ end. Thus, when **H3** is assembled into a concatenated HCR product, these two segments are colocalized through **H4**-mediated hybridization. In the attendant CHA reaction with **H5** and **H6**, segments 9 and 10 + 11 act as a toehold and a branch-migration domain, respectively (Figure 1b). In short, the correct assembly of the **H3**:**H4** concatemer via HCR is monitored via the **H5**:**H6** CHA. The formation of the **H5**:**H6** duplex can be easily detected using a fluorescent reporter named **Reporter2**, as shown in Figure 1c. As in all CHA-based circuits, the uncatalyzed hybridization of **H5** and **H6** should be extremely slow since interacting domains are sequestered in intramolecular secondary structures.

We previously observed[7] that colocalization of the two domains by direct hybridization (Figure 2a, left) leads to

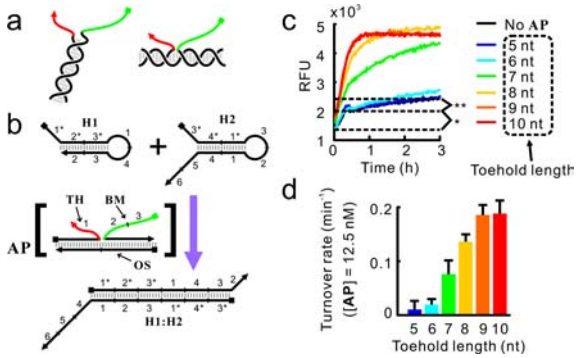

Figure 2. Feasibility of detecting the HCR product using CHA-based circuits. (a) Toehold (red) and branch-migration domain (green) colocalized by direct (left) or indirect (right) hybridization. (b) Structure of the substrates (**H1** and **H2**) and the catalyst (complex **AP**) of the CHA reaction. The toehold domain (**TH**) and branch-migration domain (**BM**) in **AP** are shown in red and green, respectively. The detailed reaction pathway is shown in Figure S2. The fluorescent reporter for **H1**:**H2**, named **Reporter**, is similar to the **Reporter2** complex shown in Figure 1c and is not shown here. (c) Kinetics of the CHA reaction catalyzed by **AP** with different toehold lengths. In all reactions, [**H1**] = 75 nM, [**H2**] = [**Reporter**] = 50 nM, [**TH**] = [**BM**] = 15 nM, and [**OS**] = 12.5 nM. Symbols * and ** denote two types of circuit leakage that are discussed further in Figure S1. (d) Turnover rate (rate of reaction divided by concentration of the catalyst) as a function of toehold length.

efficient strand displacement, and a simple reorganization of the strand placement in the DNA structure shown in Figure 2a (right) ultimately leads to the scheme shown in Figure 1b. However, this latter design should allow any two oligonucleotide sequences to be brought together by an antisense oligonucleotide (e.g., **OS** in Figure 2b) to function as a toehold (red in Figure 2a) + branch-migration domain (green in Figure 2a). The expanded generality of this scheme is now shown in several examples below. We constructed a simple DNA structure named the *a*ssembly *p*roduct (**AP**), in which the *toe*hold strand (**TH**) and the *b*ranch-*mi*gration strand (**BM**) were hybridized to the *o*rganizer *s*trand (**OS**) (Figure 2b). In essence, **OS** colocalizes the toehold domain carried by **TH** and the branch-migration domain carried by **BM**.

As shown in Figure 2c, although uncatalyzed formation of **H1**:**H2** was observable when 75 nM **H1** and 50 nM **H2** were mixed [black trace in Figure 2c, which is further dissected in Figure S1 in the Supporting Information (SI)], the presence of 12.5 nM **AP** substantially accelerated the reaction, presumably through the mechanism shown in Figure S2. Notably, the catalysis was strictly dependent on the presence of **OS**. In the absence of **OS**, the mixture of **TH** and **BM** did not yield any signal above background (Figures S1 and S3), highlighting the importance of the colocalization of the toehold and the branch-migration domain through correct DNA assembly. We further studied how temperature and toehold length (Figure 2c,d) affect the rate of CHA. These data are described in section 2 in the SI and are largely in agreement with our understanding of the kinetics of CHA reactions.[7,8]

We next determined whether we could detect multiple, different proximity junctions formed during the HCR (Figure 1a). To make the detection of the HCR product more sensitive and specific, we introduced a 12 nt oligonucleotide named **Lock** that hybridizes to the junction between segments 9 and a of **H3** (Figure 3a). The function of **Lock** is twofold: first, it

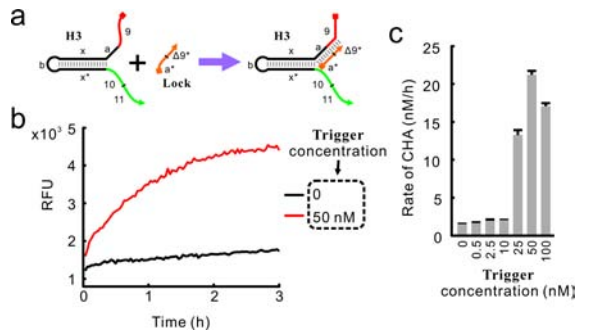

Figure 3. Detection of the HCR product using CHA circuits. (a) The **Lock** strand, which can terminate HCR reaction and abolish the activity of monomeric **H3** in catalyzing the CHA reaction. Segment Δ9* is complementary to the six nucleotides at the 3′ terminus of segment 9. (b, c) Kinetics of the CHA reactions catalyzed by HCR products at different concentrations of the **Trigger** strand.

blocks segment 'a' of **H3**, which allows timely termination of the HCR (Figure S5, lanes 8 and 16). Second, it abolishes the ability of monomeric H3 to initiate the CHA reaction by using segment 9 as a "remote toehold" (Figure S6).[9] **H3** (200 nM) and **H4** (200 nM) were incubated in the presence or absence of 50 nM **Trigger** for 16 h before saturating concentrations of **Lock** were added. When the HCR product was analyzed by native electrophoresis, high-molecular-weight HCR products were found only in the presence of **Trigger**, as expected (Figure S5). More importantly, when an aliquot of the HCR mixture was mixed with **H5**, **H6**, and **Reporter2**, the HCR with **Trigger** led to ~10-fold faster fluorescence detection of **H5**:**H6** than the HCR without **Trigger** (Figure 3b). While there was an initial burst in fluorescence (likely caused by stoichiometric opening of **H5** by the HCR product; see Figure S7), when **H6** was absent, the HCR product did not lead to a steady increase in the fluorescence signal. This observation confirmed that the HCR product indeed initiates the CHA reaction cascade catalytically.

We then repeated this experiment using various concentrations of **Trigger** (Figure 3c). Interestingly, we consistently observed several nonlinear relationships between the **Trigger** concentration and the rate of the CHA reaction (presumably reflecting the concentrations of correct assemblies formed by the HCR). For example, the rate of the CHA reaction peaked when the **Trigger** concentration was roughly one-eighth to one-fourth of the concentrations of **H3** and **H4** (which were held equal at 200 nM in all of the experiments). More **Trigger**

dx.doi.org/10.1021/ja300984b | J. Am. Chem. Soc. 2012, 134, 13918−13921

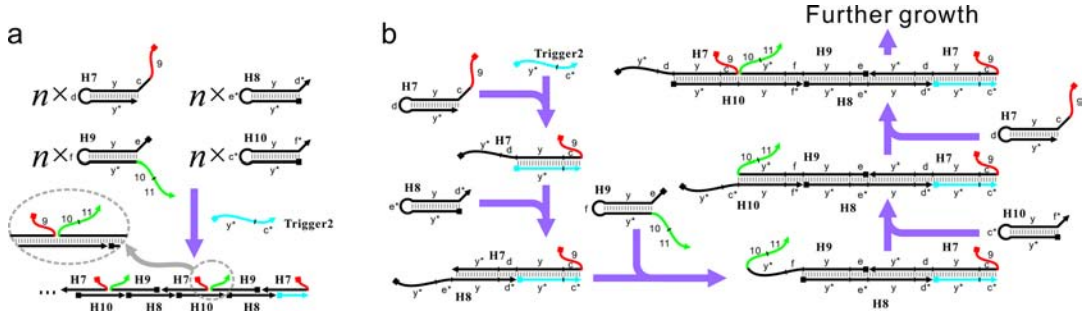

Figure 4. Sensing the assembly of a four-hairpin HCR using a CHA circuit. (a) Overall reaction of the four-hairpin HCR, where unlike **H3** (Figure 1a), the toehold (red) and branch-migration domain (green) are located on two separate molecules (**H7** and **H9**, respectively). (b) Detailed reaction mechanism of the four-hairpin HCR.

actually led to a decrease in the rate of the CHA reaction (Figure 3c and data not shown). This effect is to be expected since saturation of the initial **Trigger** should lead to the formation of very short assemblies having decreased numbers of active proximity junctions. This phenomenon was also observed via electrophoresis (Figure S5), where high concentrations of **Trigger** led to the formation of very short HCR chains.[3a]

Having shown the ability to sense the triggered reorganization of two domains (toehold and branch-migration domain) on one molecule (**H3**), we next explored whether colocalization of such domains on separate molecules could also catalyze the downstream CHA reaction. To do this, we designed a new HCR system consisting of four hairpins: **H7**, **H8**, **H9**, and **H10**. The assembly of the HCR can be initiated by the **Trigger2** strand (Figure 4). Since in this system the toehold and branch-migration domain are located on two separate molecules (**H7** and **H9**, respectively), no **Lock** is needed to suppress the basal CHA reaction catalyzed by unassembled hairpins. As before, each of the four hairpins (200 nM) and **Trigger2** (0−100 nM) were mixed for ∼24 h, after which an aliquot of the HCR mixture was mixed with **H5**, **H6**, and **Reporter2**. As can be seen in Figure 5a, 50 nM **Trigger2** led to a strong CHA signal,

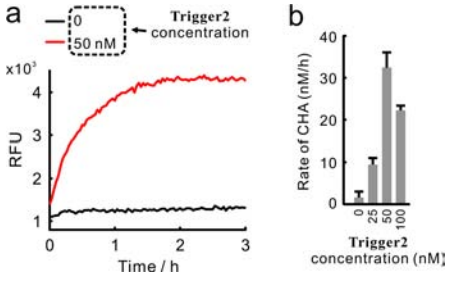

Figure 5. (a) Real-time kinetics and (b) rates of the CHA reactions catalyzed by four-hairpin HCR products at different concentrations of **Trigger2** (see Figure S8 for the gel image).

whereas the absence of **Trigger2** resulted in extremely low background. The rate of the CHA reaction was dependent on the concentration of **Trigger2** with a biphasic concentration dependence (Figure 5b) similar to that previously observed for the two-hairpin HCR (Figure 3c).

To explore further the utility of CHA circuits in structural probing, we asked whether DNA structures and CHA circuits could be designed to enable sensing of small-scale structural differences (e.g., hybridization defects). To investigate this question, we designed a CHA reaction that could potentially be accelerated by hybridization defects near the hybridization junction of the two DNA strands (Figure 6). In this structure,

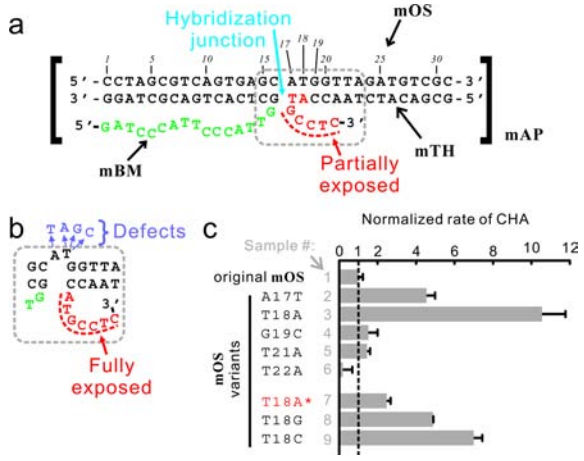

Figure 6. Detection of assembly defects using CHA circuits. (a) In the perfectly formed **mAP** structure, the toehold (shown in red) is only partially exposed. (b) Defects near the hybridization junction may fully expose the toehold. (c) Hybridization defects can be mimicked by introducing point mutations on the **mOS** strand, which stimulate the activity of mAP to different extents. T18A* (sample 7) denotes a 1:5-diluted T18A variant of **mOS**.

named *m*odified **AP** (**mAP**), the toehold and branch-migration domains (red and green in Figure 6a, carried by strands **mTH** and **mBM**, respectively) were colocalized via hybridization to the organizer strand **mOS** (Figure 6a). However, unlike the original **AP**, where the entire toehold for the CHA reaction (segment 1 in Figure 2b) was exposed, in **mAP** only five of the seven bases of the toehold (Figure 6a, red) were exposed, and the other two bases were hybridized to **mOS**. While **mAP** may be capable of triggering the CHA reaction **H1** + **H2** → **H1**:**H2**, the catalysis would be expected to be slow because of the partially sequestered toehold. By the introduction of hybridization defects between **mTH** and **mOS** near the junction, the toehold region in **mTH** should be more readily liberated (Figure 6b), which would enhance the catalytic activity of **mAP**. Unpaired bases (in this case A17 and T18) should not abolish the strand-displacement activity, and indeed, we observed that adding one or two unpaired thymidines on **OS** at the hybridization junction (Figure S9a) resulted in substantive (30−50%) residual catalytic activity of **AP** (Figure S9b,c).

In fact, single-point mutations in **mOS** near the hybridization junction (A17T, T18A, T18G, and T18C) significantly

dx.doi.org/10.1021/ja300984b | J. Am. Chem. Soc. 2012, 134, 13918−13921

enhanced the catalytic activity of **mAP** (Figure 6c, samples 2, 3, 8, and 9), while mutations further away from the hybridization junction had little or no effect (Figure 6c, samples 4−6). Thus, we have designed a circuit that can sensitively detect hybridization defects at a particular site in a nanostructure. In addition, this system exemplifies the design of a "signal on" sensor that responds to mismatches rather than perfect matches. This advance, when coupled with appropriate preamplification (e.g., polymerase chain reaction) and concentration normalization (e.g., a molecular beacon targeting an invariable region) techniques, may yield powerful genotyping tools that would be of great interest in molecular diagnostics. First, "signal on" assays in general have much higher signal-to-background ratios and consequently much higher sensitivities than "signal off" assays. For example, even when the T18A variant of **mOS** was diluted 5-fold, it still led to roughly 150% higher signal relative to the background of undiluted, original (i.e., "wild-type") **mOS** (Figure 6c, sample 7 vs 1). More importantly, in many cases multiple mutations in a small region of a gene can cause amino acid changes in the encoded protein that lead to disease or drug resistance.[10] Having the ability to respond simultaneously to multiple mutations would dramatically reduce the number of genotyping tests required to identify such genes.

The findings presented in this work have implications in both nanotechnology and molecular diagnostics. First, with proper calibration and normalization, our circuit allows fast and more readily quantifiable observation of the quantity or quality of the assembly of DNA nanostructures. Second, our methods allow HCR and CHA, two enzyme-free signal-amplification processes that have been engineered to detect both nucleic acid and non-nucleic acid analytes[3a,5,11] to be cascaded, potentially leading to greater amplification. Interestingly, although this signal amplification is larger, there are nonlinearities in the response (as shown by the output as a function of **Trigger** concentration between 10 and 25 nM in Figure 3c). This thresholding can potentially be explained by the presence of a small fraction of imperfectly formed, chain-terminating hairpins in the heterogeneous populations of **H3** and/or **H4**. These "chain terminators" are preferentially incorporated into the growing HCR chain, thus causing so-called "inhibitor ultrasensitivity"[12] (see Figure S10 for details of the proposed mechanism). This hypothesis was corroborated by our observation that the threshold was roughly proportional to the concentration of the hairpins used (data not shown). Interestingly, these insights provide another potential use for our methodology, namely, the detection of defects in oligonucleotides that will be used for the construction of complex nanostructures. This is especially important because it is becoming increasingly clear that oligonucleotide purity is an issue in both circuit and structure assembly.[13] This work, together with our earlier demonstrations,[5a,7] strongly argues for the role of CHA circuits as a reliable and general-purpose signal amplifier and suggests novel applications for assaying and quality control of nanostructure assembly.

■ ASSOCIATED CONTENT

Supporting Information

Materials and methods, effects of temperature and toehold length, Figures S1−S10, and oligonucleotide sequences. This material is available free of charge via the Internet at http://pubs.acs.org.

■ AUTHOR INFORMATION

Corresponding Author

xichen@mail.utexas.edu; andy.ellington@mail.utexas.edu

Notes

The authors declare no competing financial interest.

■ ACKNOWLEDGMENTS

This work was supported by National Institutes of Health (R01 AI092839-01, R01 GM094933-01), a National Security Science and Engineering Faculty Fellowship (FA9550-10-1-0169), and the Welch Foundation (F-1654). X.C. was partially supported by a postdoctoral trainee fellowship from Cancer Prevention Research Institute of Texas (CPRIT).

■ REFERENCES

(1) (a) Liu, J.; Cao, Z.; Lu, Y. *Chem. Rev.* **2009**, *109*, 1948. (b) Stojanovic, M. N.; Landry, D. W. *J. Am. Chem. Soc.* **2002**, *124*, 9678. (c) Cho, E. J.; Yang, L. T.; Levy, M.; Ellington, A. D. *J. Am. Chem. Soc.* **2005**, *127*, 2022. (d) Lubin, A. A.; Plaxco, K. W. *Acc. Chem. Res.* **2010**, *43*, 496. (e) Stojanovic, M. N.; Stefanovic, D. *Nat. Biotechnol.* **2003**, *21*, 1069. (f) Zhang, L.; Zhu, J.; Li, T.; Wang, E. *Anal. Chem.* **2011**, *83*, 8871.

(2) (a) Seeman, N. C. *Nano Lett.* **2010**, *10*, 1971. (b) Wilner, O. I.; Willner, I. *Chem. Rev.* **2012**, *112*, 2528. (c) Torring, T.; Voigt, N. V.; Nangreave, J.; Yan, H.; Gothelf, K. V. *Chem. Soc. Rev.* **2011**, *40*, 5636. (d) Mao, C. D.; LaBean, T. H.; Reif, J. H.; Seeman, N. C. *Nature* **2000**, *407*, 493.

(3) (a) Dirks, R. M.; Pierce, N. A. *Proc. Natl. Acad. Sci. U.S.A.* **2004**, *101*, 15275. (b) Qian, L.; Winfree, E.; Bruck, J. *Nature* **2011**, *475*, 368. (c) Zhang, D. Y. *Science* **2007**, *318*, 1121. (d) Yin, P.; Choi, H. M. T.; Calvert, C. R.; Pierce, N. A. *Nature* **2008**, *451*, 318. (e) Liu, Q. H.; Wang, L. M.; Frutos, A. G.; Condon, A. E.; Corn, R. M.; Smith, L. M. *Nature* **2000**, *403*, 175.

(4) Seeman, N. C.; Lukeman, P. S. *Rep. Prog. Phys.* **2005**, *68*, 237.

(5) (a) Li, B.; Ellington, A. D.; Chen, X. *Nucleic Acids Res.* **2011**, *39*, No. e110. (b) Choi, H. M. T.; Chang, J. Y.; Trinh, L. A.; Padilla, J. E.; Fraser, S. E.; Pierce, N. A. *Nat. Biotechnol.* **2010**, *28*, 1208.

(6) Lin, C.; Rinker, S.; Wang, X.; Liu, Y.; Seeman, N. C.; Yan, H. *Proc. Natl. Acad. Sci. U.S.A.* **2008**, *105*, 17626.

(7) Chen, X. *J. Am. Chem. Soc.* **2012**, *134*, 263.

(8) (a) Zhang, D. Y.; Winfree, E. *J. Am. Chem. Soc.* **2009**, *131*, 17303. (b) Soloveichik, D.; Seelig, G.; Winfree, E. *Proc. Natl. Acad. Sci. U.S A.* **2010**, *107*, 5393.

(9) Genot, A. J.; Zhang, D. Y.; Bath, J.; Turberfield, A. J. *J. Am. Chem. Soc.* **2011**, *133*, 2177.

(10) (a) Neumann, J.; Zeindl-Eberhart, E.; Kirchner, T.; Jung, A. *Pathol. Res. Pract.* **2009**, *205*, 858. (b) Pozzi, G.; Meloni, M.; Iona, E.; Orru, G.; Thoresen, O. F.; Ricci, M. L.; Oggioni, M. R.; Fattorini, L.; Orefici, G. *J. Clin. Microbiol.* **1999**, *37*, 1197.

(11) (a) Niu, S.; Jiang, Y.; Zhang, S. *Chem. Commun.* **2010**, *46*, 3089. (b) Shimron, S.; Wang, F.; Orbach, R.; Willner, I. *Anal. Chem.* **2012**, *84*, 1042.

(12) Ferrell, J. E. *Trends Biochem. Sci.* **1996**, *21*, 460.

(13) (a) Bois, J. S.; Venkataraman, S.; Choi, H. M.; Spakowitz, A. J.; Wang, Z. G.; Pierce, N. A. *Nucleic Acids Res.* **2005**, *33*, 4090. (b) Zhang, D. Y.; Winfree, E. *Nucleic Acids Res.* **2010**, *38*, 4182.